Comparative Analysis of Small Secreted Peptide Signaling during Defense Response: Insights from Vascular and Non-Vascular Plants

Irina Lyapina[1], Daria Ganaeva[1], Eugene A. Rogozhin[1,2], Ekaterina V. Ryabukhina[1], Dmitry Yu. Ryazantsev[1], Anna Mamaeva[1] and Igor Fesenko[1*]

[1]Shemyakin-Ovchinnikov Institute of Bioorganic Chemistry, Miklukho-Maklaya 16/10, 117997 Moscow, Russia

[2]All-Russian Institute for Plant Protection, Pushkin 196608, Russia

*Corresponding author

Abstract

Peptides play a crucial role in regulating plant responses to stress conditions. Small secreted peptides (SSPs) are known to be involved in immune response and are found in all land plants. However, the evolution of stress peptide signaling remains poorly understood. Here, we compared the pathogen-induced transcriptomes of the moss *Physcomitrium patens*, *Zea mays*, *Brassica napus*, and *Solanum tuberosum* to gain insight into the role of established SSP families from vascular and non-vascular plants in immune response. We identified 50, 76, 135, and 309 known SSP genes, differentially expressed during infection, in *P. patens*, *S. tuberosum*, *Z. mays,* and *B. napus*, respectively. In addition, a novel family of bryophyte-specific PSY-like peptides that are differentially regulated under infection was identified. The similarity of SSPs across the examined plant species was validated through a comparative analysis of peptide motifs and predicted three-dimensional structures. However, despite the similar patterns of antimicrobial peptide expression, only the RALF peptide family was differentially regulated under infection in both vascular and non-vascular plants. We also found that EPFL peptides, which are involved in growth and development processes in angiosperms, were differentially regulated in *P. patens* in response to pathogen infection. Thus, our study showed the complex nature of SSP signaling and shed light on the regulation of SSPs in different plant lineages during infection.

Introduction

Peptides regulate different processes, including the response to stress conditions (Hou et al., 2021; Lyapina et al., 2019; Olsson et al., 2019). Like animal cytokines (J.-M. Zhang & An, 2007), a group of plant peptides modulating immune response was named "phytocytokines" (Hou et al., 2021). The most characterized phytocytokines include PLANT ELICITOR PEPTIDES (PEP), PAMP-INDUCED PEPTIDES (PIPs), RAPID ALKALINIZATION FACTOR (RALF), PHYTOSULFOKINES (PSKs), PLANT PEPTIDE CONTAINING SULFATED TYROSINE1 (PSY1), SERINE-RICH ENDOGENOUS PEPTIDES (SCOOPs), GOLVENs (GLVs), CLAVATA3/EMBRYO SURROUNDING REGION (CLV3/CLE), CLAVATA3/EMBRYO SURROUNDING REGION (CLV3/CLE) and INFLORESCENCE DEFICIENT IN ABSCISSION (IDA) families (Rzemieniewski & Stegmann, 2022). In addition to the stress response, phytocytokines are shown to be involved in the regulation of plant growth and development (Hou et al., 2021).

Besides phytocytokines, antimicrobial peptides (AMPs) play an important role in plant defense, triggering pathogen cell lysis due to lipid membrane disruption (Moravej et al., 2018). Plant AMPs are small, cysteine-rich proteins (Kulaeva et al., 2020; Tam et al., 2015) that have diverse structures, characteristics, and action mechanisms. The classification of plant AMPs is mostly based on sequence similarity and structures. The most characterized AMPs include thionins, defensins, hevein-like peptides, knottins, stable-like peptides, lipid transfer proteins, snakins, and cyclotides (Lima et al., 2022). Antimicrobial peptides were found in most plant taxa.

The phytocytokines, antimicrobial peptides, and plant peptide hormones that control growth and development are often referred to as Small Secreted Peptides (SSPs). The plant SSPs are involved in cell-to-cell communications and share common features: 1) the active peptide sequences are embedded at the C-terminus of 100–250 aa functional or non-functional protein precursors; 2) protein precursors contain a hydrophobic N-terminal secretion signal; 3) peptides are released by specific proteases in certain conditions (de Bang et al., 2017; Hu et al., 2021). Nevertheless, precursors of widely recognized phytocytokines, including systemin (SYS) and PEP precursors, do not possess an export signal, which highlights the shortcomings

58 of the SSP classification (Hu et al., 2021; Tavormina et al., 2015). The group of SSPs consists
59 of post-translationally modified (PTM) peptides, cysteine-rich peptides (CRP), and non-Cys-
60 rich and non-PTM peptides. The families of PTM peptides such as PSK, PSY,
61 RGF/GLV/CLEL, CLE, and IDA are widely conserved and were presented in the most recent
62 common ancestor of angiosperms and bryophytes. The cysteine-rich peptides, such as RALF,
63 EPIDERMAL PATTERNING FACTOR (EPF), and EPF-LIKE (EPFL), are shown to be
64 involved in the regulation of many aspects of plant growth and development (Tian et al., 2022).
65 These families were also present in the most recent common ancestor of angiosperms and
66 bryophytes (Furumizu & Shinohara, 2024). The families of systemin (SYS) and PEP peptides
67 are the most well-known phytocytokines, not belonging to the aforementioned two categories.

68 During the past decade, thousands of SSPs belonging to more than 70 families have
69 been identified in different plant genomes (Boschiero et al., 2020). In *Triticum aestivum*, 4,981
70 putative SSPs were identified, among which 1,790 SSPs were grouped into 38 known SSP
71 families (Tian et al., 2022). In *Oryza sativa* 236 SSPs, including 52 previously unannotated,
72 were shown to be involved in the immune response (P. Wang et al., 2020). In *Medicago*
73 *trancatula*, 4439 genes were predicted to encode SSPs (Boschiero et al., 2020). The
74 bioinformatic search in three bryophyte lineages — mosses, liverworts, and hornworts
75 identified hundreds of SSPs, confirming the important role of peptide signaling in all plant
76 lineages (Lyapina et al., 2021).

77 The databases of plant SSPs, such as PlantSSP (Ghorbani et al., 2015), OrysSSP (Pan
78 et al., 2013), and MtSSPdb (Boschiero et al., 2020) have been published in recent years.
79 Nevertheless, the catalogue of plant SSPs is far from complete, and new peptide families are
80 still being discovered. Recently, the new family of plant phytocytokines, SCREW/CTNIP, was
81 identified in Arabidopsis based on analysis of stress-induced transcriptomes (Z. Liu et al.,
82 2022; Rhodes et al., 2022). Moreover, plant genomes contain tens of thousands of small open
83 reading frames (smORFs, < 100 aa) that can encode unannotated secreted peptides or be a raw
84 material for the evolution of novel SSPs (Fesenko et al., 2021; Hanada et al., 2013). Such
85 translatable smORFs can be located on transcripts that were annotated as long non-coding
86 RNAs (lncRNAs) (Hsu & Benfey, 2018).

87 The evolution and role of SSPs in land colonization by plants is currently being
88 discussed (Bowman, 2022; Bowman et al., 2017; Ghorbani et al., 2015). The analysis of

89 phytocytokines in different plant groups showed that most of them are family- or species-
90 specific. That probably reflects their fast evolution, which is driven by arms races between
91 plants and microbes. For example, a SCOOP family is specific to *Brassicaceae* family (Yang
92 et al., 2023). Systemin and hydroxyproline-rich systemin were identified only in *Solanaceae*
93 family (Ryan & Pearce, 2003). The PEP family is present in many angiosperm families, but
94 their sequences are highly divergent (Lori et al., 2015; Tanaka & Heil, 2021). A species-
95 specific *Z. mays* immune signaling peptide 1 (Zip1) was found in *Zea mays* (Ziemann et al.,
96 2018). Nevertheless, such PTM phytocytokine families as PSK, PSY, RGF/GLV/CLEL, CLE,
97 and IDA were probably present in the most recent common ancestor of angiosperms and
98 bryophytes (Furumizu & Shinohara, 2024). The most phytocytokines were identified in
99 angiosperms. However, the role of RALF peptides in the immune response was recently
100 demonstrated in the moss *P. patens* (Mamaeva et al., 2023). Nevertheless, it is currently unclear
101 if plant lineages such as bryophytes, lycophytes, ferns, and gymnosperms contain unannotated
102 peptide families regulating response to stress conditions. Moreover, the interplay of different
103 families of phytocytokines in different plant lineages is poorly understood. For example, the
104 understanding of the interaction between several families of phytocytokines in the immune
105 response in diverse plant lineages is currently incomplete.

106 In this study, we aimed to compare patterns of SSP expression under pathogen invasion
107 in vascular and non-vascular plants. We performed comparative analysis of pathogen-induced
108 transcriptomes of three angiosperm species - *Zea mays*, *Brassica napus*, and *Solanum*
109 *tuberosum,* and one bryophyte — the moss *Physcomitrium patens*. Our analysis revealed
110 different patterns of SSP transcription between vascular plants as well as between vascular and
111 non-vascular plants. In addition, our bioinformatic search identified two novel putative peptide
112 families, specific to bryophytes.

113

Materials and Methods

Pre-processing

Raw RNA-sequencing data of the following plants under biotic stress were analyzed: model organism moss *Physcomitrium patens*, and angiosperm plants: *Zea mays*, *Brassica napus*, *Solanum tuberosum* (accessions: SRP274010, SRP390856, SRP053361, SRP066006). Three biological replicates for mock and infection samples were sequenced using Illumina HiSeq2000. The following infection time points were chosen: 4, 8 and 24 hours post inoculation (hpi) for moss *P. patens* infected by *Botrytis cinerea*, for angiosperms – 24, 40, 60 hpi for *Z. mays* infected by *Colletotrichum graminicola;* 24, 48, 96 hpi for *B. napus* infected by *Sclerotinia sclerotiorum*; 12, 24, 72 hpi for *S. tuberosum* infected by *Pectobacterium carotovorum.*

FastQC (Andrews, 2010) was used for quality control, Trimmomatic (Bolger et al., 2014) was used to clip adapters and nucleotides of low quality. Genomes and genome annotations were accessed via Phytozome (https://phytozome-next.jgi.doe.gov/, Goodstein et al., 2012) and Ensembl Plants (https://plants.ensembl.org/). *P. patens* v3.3, *Z. mays* Ref_Gen_V4, *B. napus* AST_PRJEB5043_v1, and *S. tuberosum* v6.1 versions were selected.

Assembly and ORF prediction

Genomes were indexed using hisat2-build, reads were mapped to the reference genome using HISAT2 (Kim et al., 2015). Samtools (H. Li et al., 2009) was used for collecting mapping statistics.

De novo transcripts assembly was done using Stringtie (Pertea et al., 2015), Stringtie -e mode was applied for quantification. Prediction of open reading frames (ORFs) from AUG start codon for assembled transcripts with further automatic translation to amino acid sequences of length over 30 aa was done using orfipy (Singh & Wurtele, 2021). The longest ORF per transcript was selected, considering that the longest ORF represents actual coding sequence.

Functional annotation

Interproscan (Quevillon et al., 2005) was used to predict protein domains. Analysis of homology with known families of small secreted peptides (SSPs) was done using the SSP

141 prediction tool (https://mtsspdb.zhaolab.org/prediction/, Boschiero et al., 2020). Plant long non-
142 coding RNAs were accessed via PLncDB (https://www.tobaccodb.org/plncdb/).

143 DE analysis and filtration

144 Differential gene expression analysis was done using the edgeR package (Robinson et al.,
145 2010). Transcripts with 1 > logFC < -1 and FDR < 0.05 were considered differentially expressed.

146 Translated ORFs of length less than 200 amino acids were considered small ORFs
147 (smORFs). ORFs predicted as known SSPs by SSP prediction tool were assigned to the
148 corresponding SSP family based on homology to SSPs from other plants. Search for potential
149 novel candidates of signaling peptides was performed in smORFs corresponding to DE transcripts,
150 with predicted signal sequence, no transmembrane or known protein domains, and with no
151 homology to known SSPs from other plants.

152 Sequence alignment and structure prediction

153 Multiple sequence alignments (MSAs) were created using the high precision L-INS-I
154 algorithm of MAFFT v7 (Katoh & Standley, 2013). Alignments were visualized using JalView
155 v2.11.2.2, Clustalx color (Waterhouse et al., 2009).

156 Prediction of three-dimensional structures was done using AlphaFold2 (Jumper et al.,
157 2021). Structural comparison was performed using TM align (Y. Zhang & Skolnick, 2005). Such
158 metrics as RMSD and TM-score were considered. Structural search against PDB and AlphaFold
159 database (AFDB) was performed using Foldseek (van Kempen et al., 2024).

160 Search for homologs

161 Search for paralogs of novel immune peptide candidates was performed using BLASTP
162 against all major ORFs assigned for each transcript. Hits with E-value < 0.00001 were considered
163 significant. Search for orthologs and paralogs for novel candidates in other databases was done
164 using NCBI BLASTP against non-redundant protein sequences database, organism: *Viridiplantae.*
165 Sequences with no matches or with matches to unannotated proteins ("putative", "unknown",
166 "uncharacterized", etc) were selected. TBLASTN against 1000 plant transcriptomes (1KP,
167 https://db.cngb.org/datamart/plant/DATApla4/) was run to search for homologs of novel
168 candidates among translated nucleotide sequences of other plants published in 1KP. The following

169 default parameters were customized: 250 max. target sequences, word size 3. Hits with E-value <
170 0.01 were considered significant.

171 Cloning and recombinant protein expression

172 The pET32b+ vector ("Novagen", USA) was used for recombinant plasmids construction.
173 When the obtained recombinant plasmid is expressed, a hybrid protein is created, that contains
174 thioredoxin, polyhistidine domain, enteropeptidase cleavage site (DDDDR) and the peptide
175 sequences. Previously an assembly of synthetic genes encoded MEG and EPFL peptides was
176 carried by PCR method. This procedure was made according to Shevchuk et al. (2004): the long
177 oligonucleotides (Supplementary Table 1) (100 ng of each) and all required components were
178 added to PCR mixture (the Phusion HS II DNA polymerase was used). The PCR amplification
179 was carried out in using with the following program: 94 ◦C – 60 s; 94 ◦C – 20 s, 60 ◦C – 20 s, 72
180 ◦C – 20 s – 10 cycles; 72 ◦C – 60 s. Then 2.5 µl from the obtained mixture was added to a novel
181 amplification mixture containing flanking for the corresponding peptides oligonucleotides for (0.5
182 µM of each), and the amplification was carried out according to the same program (20 cycles).
183 The PCR product was purified from the agarose gel and cloned into the pET32b+ vector by using
184 HihdIII/KpnI restriction endonucleases. The obtained construction was transformed into *E. coli*
185 strain Origami. The induction and purification of the recombinant protein was carried out under
186 native conditions according to the QIAexpressionist manual ("Qiagen", Germany). For the
187 purpose of fusion protein purification from bacterial cells 1000 ml LB growth medium was
188 inoculated by 25 ml of overnight *E. coli* culture. The induction was carried out for 4 h in the
189 presence of 1 mM IPTG, then the cells were centrifuged, and the precipitate was resuspended in
190 50 ml of buffer A (50 mM NaH2PO4, 300 mM NaCl, 10 mM imidazole, pH 8.0). The *E. coli* cells
191 disruption was realized for 30 min at ice with addition of lysozyme (1 mg/ml) followed by
192 sonication. The clarified cell lysate was applied to Ni-NTA agarose column (10 ml) that was
193 preliminarily equilibrated by buffer A, then the column was washed by buffer A containing 20
194 mM imidazole. The fusion protein was eluted by buffer B (50 mM NaH2PO4, 300 mM NaCl, 250
195 mM imidazole, pH 8.0). The purity and size of recombinant hybrid proteins was evaluated by
196 SDS-PAGE electrophoresis.

197 Plant growth

198 Protonemata of *Physcomitrium patens* subsp. patens Gransden 2004 (Freiburg, Germany)
199 were grown in 100 mL liquid Knop medium containing 500 mg/L ammonium tartrate under white
200 light with a photon flux of 61 μmol/m2 s under a 16-hour photoperiod at 24°C. Seven-day-old
201 protonema was used for analysis.

202 **ROS detection**

203 For intracellular ROS detection we used the fluorescent dye 2′,7′-Dichlorofluorescin
204 Diacetate (DCFH-DA, Sigma-Aldrich, USA). *P. patens* protonemata was treated with 5 μM
205 synthesized PpEPFL or PpMEG for 10 min. Samples were incubated with 10 μM DCFH-DA for
206 15 min. The detection was performed on the fluorescent microscope Axio Imager M2 (Zeiss) with
207 an AxioCam 506 mono digital camera and filter units. The No. 44 filter (λex BP 475 nm/40 nm;
208 λem BP 530 nm/50 nm) was used for DCFH-DA fluorescence detection. The exposure was set to
209 300 msec, FITC and Brightlight channels were used. Data on the fluorescence intensity were
210 obtained from the related Zeiss software Zen.

211

212 # Results

213 ## Identification of SSPs in pathogen-induced transcriptomes

214 In order to analyze expression patterns of known and previously unannotated SSPs
215 during immune response, we re-analyzed four published transcriptomes of phylogenetically
216 distant species: the moss *Physcomitrium patens* (Physcomitrella), *Zea mays*, *Brassica napus*,
217 and *Solanum tuberosum* (Kwenda et al., 2016; Reboledo et al., 2021; D. Wang et al., 2022; Xia
218 et al., 2023; Figure 1A). These transcriptomes were selected based on the following criteria: 1)
219 the plants were infected with either necrotrophic or hemibiotrophic pathogens; 2) the quality
220 of raw data (see Methods); and 3) RNA-seq analysis was performed at different time points
221 after pathogen inoculation.

222 The RNA-seq reads were re-mapped to the corresponding genomes with the following
223 alignment rate: 91% for *P. patens*; 96% for *Z. mays*; 83% for *B. napus*; and 85% for *S.*
224 *tuberosum*. Overall, we identified from 28,234 to 67,590 transcripts at different hpi (hours post
225 infection) across all selected species (Figure 1B). The following number of transcripts were
226 assigned to annotated genes: 23,843 for *P. patens*; 15,269 for *S. tuberosum*; 15,138 for *Z. mays*
227 and 19,875 for *B. napus*. To annotate all assembled transcripts, open reading frames (ORFs)
228 larger than 30 amino acids (aa) that start with AUG codons were predicted using orfipy tool
229 (Singh & Wurtele, 2021). For annotation, the major ORF was selected for each transcript,
230 resulting in approximately 45,000 predicted proteins in *P. patens* and *S. tuberosum*;
231 approximately 40,000 and 60,500 predicted proteins in *Z. mays* and *B. napus*, respectively.

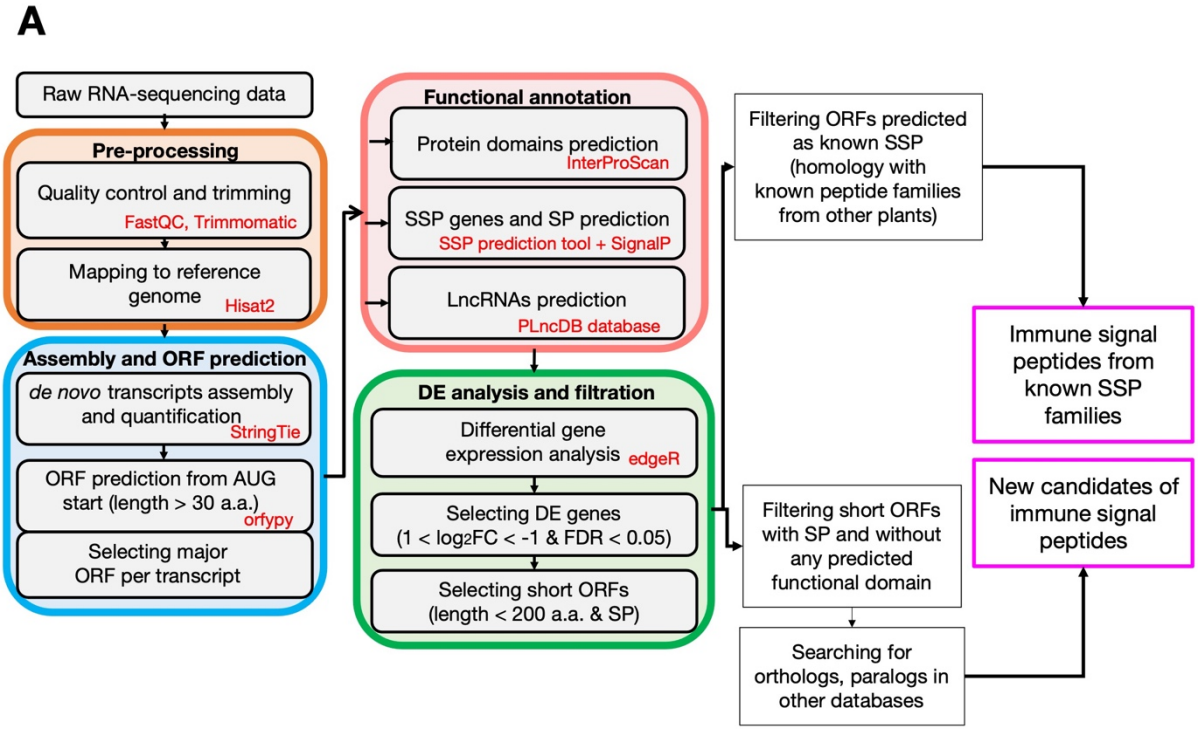

B

Plant	*Physcomitrium patens*			*Zea mays*			*Solanum tuberosum*			*Brassica napus*		
Pathogen	*B.cinerea*			*C. graminicola*			*P. carotovorum*			*S. sclerotiorum*		
Time Point, h	**4**	**8**	**24**	**24**	**40**	**60**	**12**	**24**	**72**	**24**	**48**	**96**
Transcripts	43780	43861	43978	42208	41277	28234	48590	49887	49434	65613	66116	67590
DE transcripts (% lncRNA)	251 (0.4)	6256 (0.21)	13190 (0.17)	18129 (0.41)	8572 (0.36)	9685 (0.41)	2266 (0.75)	704 (0.85)	1900 (1.05)	7938 (0.38)	10523 (0.29)	15143 (0.32)
DE short ORF + SP (% lncRNA)	2 (0)	172 (0.6)	348 (0.57)	1184 (0.34)	698 (0.14)	987 (0.61)	296 (1.35)	109 (3.7)	240 (1.25)	633 (0.32)	1121 (0.27)	1535 (0.52)
DE SSP	2	27	38	53	35	48	42	14	20	70	99	140
All SSP	129	129	129	89	94	92	174	174	157	314	289	250

Figure 1. A - General scheme of work pipeline; **B -** transcripts assembly statistics.

The predicted proteins were then annotated using the InterProScan tool (Quevillon et al., 2005). This resulted in assigning to known protein domains about 57% of assembled transcripts in *P. patens* and *B. napus*, 53% in *S. tuberosum* and 70% in *Z. may*. Among the

237 most represented domains, such as chloroplast- or ribosome-related, a significant part of
238 predicted ORFs belonged to uncharacterized domains or were unannotated (Supplementary
239 Table 2).

240 We next used the online SSP prediction tool (https://mtsspdb.zhaolab.org/prediction/,
241 Boschiero et al., 2020) to determine the transcripts encoding precursors of known SSP families
242 (Figure 1B; Supplementary Table 3). Overall, 129, 92, 168, and 284 transcripts encoding
243 potential SSP precursors were identified in the assembled transcriptomes of *P. patens*, *Z. mays*,
244 *S. tuberosum*, and *B. napus*, respectively (Figure 1B; Supplementary Table 3).

245 For each species, we next identified differentially expressed (DE) transcripts ($-1 \leq \log2$
246 fold change ≥ 1, $P\text{adj} < 0.05$) at each time point (Table 1B; Supplementary Table 2). In *P.*
247 *patens* and *Z. mays*, the highest number of DE transcripts was found at 24 hpi - 30% and 43%
248 of all transcripts, respectively (Figure 1B; Supplementary Table 2). For *S. tuberosum* the largest
249 number of DE transcripts was found at 12 hpi (4.7 % of overall transcripts), and for *B. napus* -
250 at 96 hpi (22.4% of overall transcripts) (Figure 1B; Supplementary Table 2).

251 We additionally identified lncRNAs in assembled transcriptomes that could potentially
252 encode for unannotated peptide precursors (Hsu & Benfey, 2018). To estimate the proportion
253 of lncRNAs in differentially regulated transcripts, we selected the assembled transcripts that 1)
254 do not code for annotated proteins; 2) do not assign to known SSP families; 3) contain smORFs
255 below 100 codons; and 4) do not overlap known genes on the same strand. We annotated such
256 transcripts using the lncRNA database PLncDB (https://www.tobaccodb.org/plncdb/). At each
257 time point, lncRNA transcripts accounted for approximately 0.17–1.05% of differentially
258 regulated transcripts in each species, with *S. tuberosum* having a higher percentage and *P.*
259 *patens* having a lower one (Figure 1B; Supplementary Table 2). We suggest that it can be the
260 result of both biological and technical reasons.

261 For further analysis, we selected 50, 76, 135, and 309 SSP genes, differentially
262 expressed during infection, in *P. patens*, *S. tuberosum, Z. mays* and *B. napus*, respectively
263 (Figure 1B; Supplementary Table 3). Moreover, we additionally selected DE transcripts, which
264 code for unannotated proteins $\leq$ 200 aa, containing N-terminal signals (Figure 1B;
265 Supplementary Table 2). The corresponding predicted proteins were used for the identification
266 of novel, previously unannotated peptide families. Some of them were classified as long
267 noncoding RNAs (Figure 1B; Supplementary Table 2).

Transcriptional patterns of SSP genes in different plant lineages

We next analyzed the transcriptional patterns of different groups of SSPs in response to phytopathogen infection. The first group consists of selected known phytocytokines. The second group included "peptide hormones," which have been demonstrated to control growth and development but not stress responses. The third group consists of known families of AMPs.

The transcriptional regulation of phytocytokines

The most common differentially regulated phytocytokines in all examined species were from conserved phytocytokine families such as PSK, CLE, PSY, and RALF. The transcripts that encode RALF peptides were identified in all examined species at three time points. The members of this family were differentially regulated under infection in *P. patens*, *B. napus* and *Z. mays*. In *P. patens*, the PpRALF1 (Pp3c3_15280) gene was significantly up-regulated under infection (Figure 2; Supplementary Table 3). Some members of the RALF family were significantly down-regulated under infection in *B. napus* and *Z. mays* (e.g., CDX78035 in *B. napus* and Zm00001d033941_T001 in *Z. mays*; Figure 2).

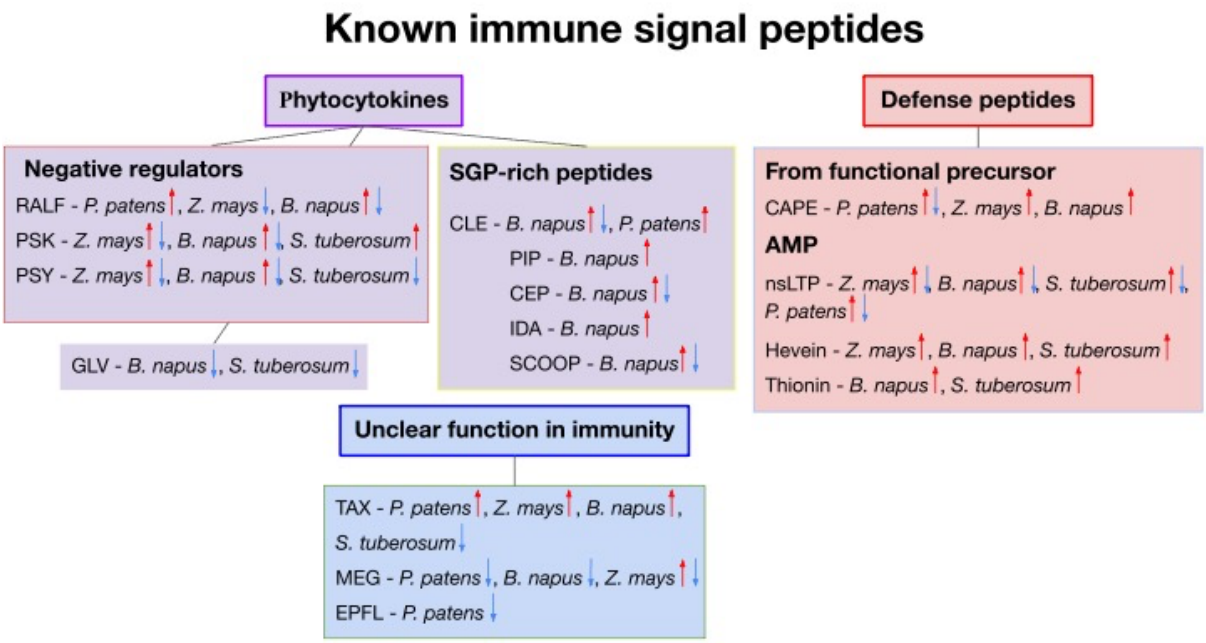

285 **Figure 2.** Groups of differentially expressed gene families predicted as known SSPs involved
286 in immunity. Red arrows indicate up-regulated transcripts, blue arrows - down-regulated.

287 Previously, PSK peptides were shown to regulate the immune response to biotrophic
288 and necrotrophic pathogens in an antagonistic manner in Arabidopsis (Y. Li et al., 2024). The
289 genes belonging to the PSK family were differentially regulated in vascular plants but not in
290 *P. patens*. In Z. *mays*, PHYTOSULFOKINES 6-RELATED gene (Zm00001d023385_T001)
291 was up-regulated during infection. In addition, another phytosulfokine gene
292 (Zm00001d023384_T001) was up- and down-regulated at different hpi, and
293 Zm00001d048006_T001 was down-regulated. In *B. napus*, we identified 22 up-regulated
294 transcripts of PSK genes, and two genes, CDX68551 and CDY36518, were down-regulated.
295 One PSK gene (Soltu.DM.02G027440.2) was upregulated in *S. tuberosum* (Figure 2;
296 Supplementary Table 3).

297 The PSY family was recently shown to play a role in regulating the trade-off between
298 plant growth and stress response in vascular plants (Ogawa-Ohnishi et al., 2022). PSY
299 receptors (PSYRs) activate the expression of various genes encoding stress response
300 transcription factors upon detection of the ligands (Ogawa-Ohnishi et al., 2022). We found that
301 PSY transcripts were significantly down-regulated in all vascular plants under infection:
302 MSTRG.18847.1 in *S. tuberosum*; CDY71288, CDX80347 and MSTRG.42712.1 in *B. napus*;
303 14 transcripts in *Z. mays* (Figure 2; Supplementary Table 3). Some PSY genes in *Z. mays* and
304 *B. napus* were also up-regulated: Zm00001d038523_T001, Zm00001d020443_T001,
305 MSTRG.18595.2 and MSTRG.17209.2 in *Z. mays*; CDY64688, CDY35659, CDY69338 and
306 MSTRG.43937.2 in *B. napus* (Figure 2; Supplementary Table 3). However, our analysis did
307 not detect the transcript of the PSY gene in P. *patens*.

308 The analysis of phytocytokines specific to vascular plants showed that PIP (7 up-
309 regulated transcripts, 3 annotated: two isoforms of CDY38932 and CDX96041), CEP (12 up-
310 regulated transcripts, 3 annotated: CDY50603, CDX93232 and CDY63206; one down
311 MSTRG.44689.1), IDA (CDY08563), and SCOOP (three up-regulated: MSTRG.37091.1,
312 MSTRG.4039.1 and MSTRG.4077.1; one down-regulated MSTRG.30356.2) peptides were
313 significantly up-regulated, and some down-regulated, in *B. napus* (Figure 2; Supplementary
314 Table 3).

315 Transcripts of IDA peptide precursors were detected in *S. tuberosum* plants, but their
316 transcription did not show significant changes under infection.

317 Transcripts of PEP precursors (PROPEPs) were not detected in our analysis across the
318 examined plant species, likely due to their low transcription levels.

319 Thus, our analysis showed that only the RALF peptide family was differentially
320 regulated under infection in vascular and non-vascular plants.

321 **The transcriptional patterns of known peptide growth hormones**

322 The number of SSP families that were shown to regulate only growth and development
323 processes is limited. For example, EPIDERMAL PATTERNING FACTOR (EPF) and EPF-
324 LIKE (EPFL) family play a role in regulating plant growth and development (Y. He et al.,
325 2023; Xiong et al., 2022). Recently, the EPFL family was found to be significantly down-
326 regulated upon *F. oxisporum* infection and elicitor treatments in tomato (Slezina et al., 2021).
327 Our analysis revealed transcripts encoding members of the EPFL family in all angiosperms,
328 although their transcription level remained unchanged during infection. However, we found
329 that some members of EPFL family were significantly down-regulated in the moss *P. patens*.
330 According to our analysis, 14 transcripts belonging to the EPFL peptide family were identified
331 in *P. patens*. From them, 9 transcripts were significantly down-regulated (six annotated genes:
332 Pp3c6_12270, Pp3c23_5720, Pp3c24_9860, Pp3c23_11350, Pp3c1_26030, Pp3c6_27020;
333 Figure 2; Supplementary Table 3). The function of this peptide family in bryophytes is
334 currently unknown. To this end, we measured the accumulation of intracellular reactive oxygen
335 species (ROS) in moss protonemata after treatment with 5 μM synthetic EPFL (Pp3c6_12270)
336 for 10 min. The treatment resulted in a significant accumulation of ROS compared to the
337 control (paired t-test: *P-value* < 0.0005; Supplementary Figure 1A). Thus, these results suggest
338 that moss EPFL peptides may be involved in the regulation of the immune response, as has
339 been recently shown in tomato (Slezina et al., 2021).

340 The genes encoding members of the cysteine-rich TAX (TAXIMIN) family peptide
341 were significantly up-regulated in *Z. mays* (four transcripts, three isoforms of
342 Zm00001d008923_T001 and one not annotated MSTRG.18593.1), *B. napus* (seven transcripts,
343 two annotated: CDY31955 and CDY19064), *P. patens* (Pp3c4_17790) and down-regulated in

344 *S. tuberosum* (MSTRG.21268.1; Figure 2 Supplementary Table 3). This family was suggested
345 to play a role in nutrient-status-related signaling (de Bang et al., 2017).

346 Another peptide family of cysteine-rich peptides, MEG (Maternally Expressed Gene),
347 was previously shown to be down-regulated in tomato plants under infection (Slezina et al.,
348 2021). We found that members of this family were significantly down-regulated in *P. patens*
349 (two isoforms of Pp3c5_6640) and *B. napus* (MSTRG.22520.1) and some members were
350 significantly up- and down-regulated in *Z. mays* (three up-regulated transcripts: two isoforms
351 of Zm00001d005037_T001 and Zm00001d052375_T002; two down-regulated transcripts:
352 Zm00001d052375_T002 and Zm00001d042365_T001; Figure 2 Supplementary Table 3).
353 Since the functions of this peptide in bryophytes are also unknown, we synthesized MEG from
354 moss *P. patens* and measured the accumulation of ROS molecules in moss protonema cells
355 after treatment with 5 µM PpMEG, although no significant differences from the control were
356 observed (Supplementary Figure 1B).

357 TPD 1 (TAPETUM DETERMINANT 1) is a secreted cysteine-rich small protein that
358 was shown to control anthers cell differentiation in Arabidopsis (Huang et al., 2016). We
359 identified two TPD transcripts in the moss *P. patens* (STRG.20746.1, STRG.20746.2) and
360 three of the five transcripts encoded TPD-like peptides in *Z. mays* (two of them already
361 annotated (Zm00001d049823_T001, Zm00001d006677_T001) were significantly up-
362 regulated (Supplementary Table 3).

363 Thus, our analysis shows that cysteine-rich peptides, which were not shown to play a
364 role in regulating immune responses, were actively regulated during infection in all plant
365 lineages. Our findings show that the widely conserved RALF and EPFL peptide families may
366 play a role in the immune response in both vascular and non-vascular plants.

367 The transcriptional regulation of antimicrobial SSPs

368 We identified several different SSPs classified as antimicrobial and protease inhibitors
369 in the analyzed species, such as Gibberellic acid-stimulated Arabidopsis (GASA), ARACIN,
370 Potato type II proteinase inhibitor, SubIn and others. The most known antimicrobial peptides,
371 hevein and thionin, were identified in the transcriptomes of all examined species
372 (Supplementary Table 3). However, hevein transcripts were significantly up-regulated during
373 infection only in vascular plants (Figure 2; Supplementary Table 3). Thionins were

374 significantly up-regulated in *B. napus* and *S. tuberosum*, but we did not identify differential
375 expression in other species.

376 The Non-specific lipid transfer proteins (nsLTP) are a plant-specific superfamily of
377 cysteine-rich AMPs (Santos-Silva et al., 2023). The transcripts of nsLTP genes were identified
378 in all analyzed plant species and were the most highly represented group of transcripts, both
379 up- and down-regulated (Supplementary Table 3). Our findings showed that nsLTP have
380 similar patterns of regulation in the response to pathogen attack in vascular and non-vascular
381 plants (Figure 2).

382 Comparative analysis of SSP motifs

383 We next compared the peptide motifs of bryophyte and angiosperm SSPs, differentially
384 regulated in the transcriptomes of the examined species. The SSPs were selected based on the
385 following criteria: 1) differentially expressed in *P. patens* and in at least one angiosperm
386 species; or 2) differentially expressed in *P. patens*. We used only functional peptide sequences
387 for this analysis (Figure 3A; Supplementary Figure 2).

388 The EPFL peptides identified in *P. patens*, *S. tuberosum*, and *B. napus* revealed a
389 typical cysteine pattern as well as a conserved GS region (Figure 3A, Supplementary Figure
390 2A), which is similar to the previous studies (Takata et al., 2013; Xiong et al., 2022).

391 The YISY motif, which is shown to play a role in receptor binding (R. Zhang et al., 2023), was
392 identified in most RALF peptides from *P. patens*, *S. tuberosum,* and *B. napus*. However, *Z.*
393 *mays* peptides contain an ISY motif (Figure 3A, Supplementary Figure 2B). The RGC region
394 was found in all studied plants, suggesting that RALF peptides share known motifs in all
395 examined species (R. Zhang et al., 2023).

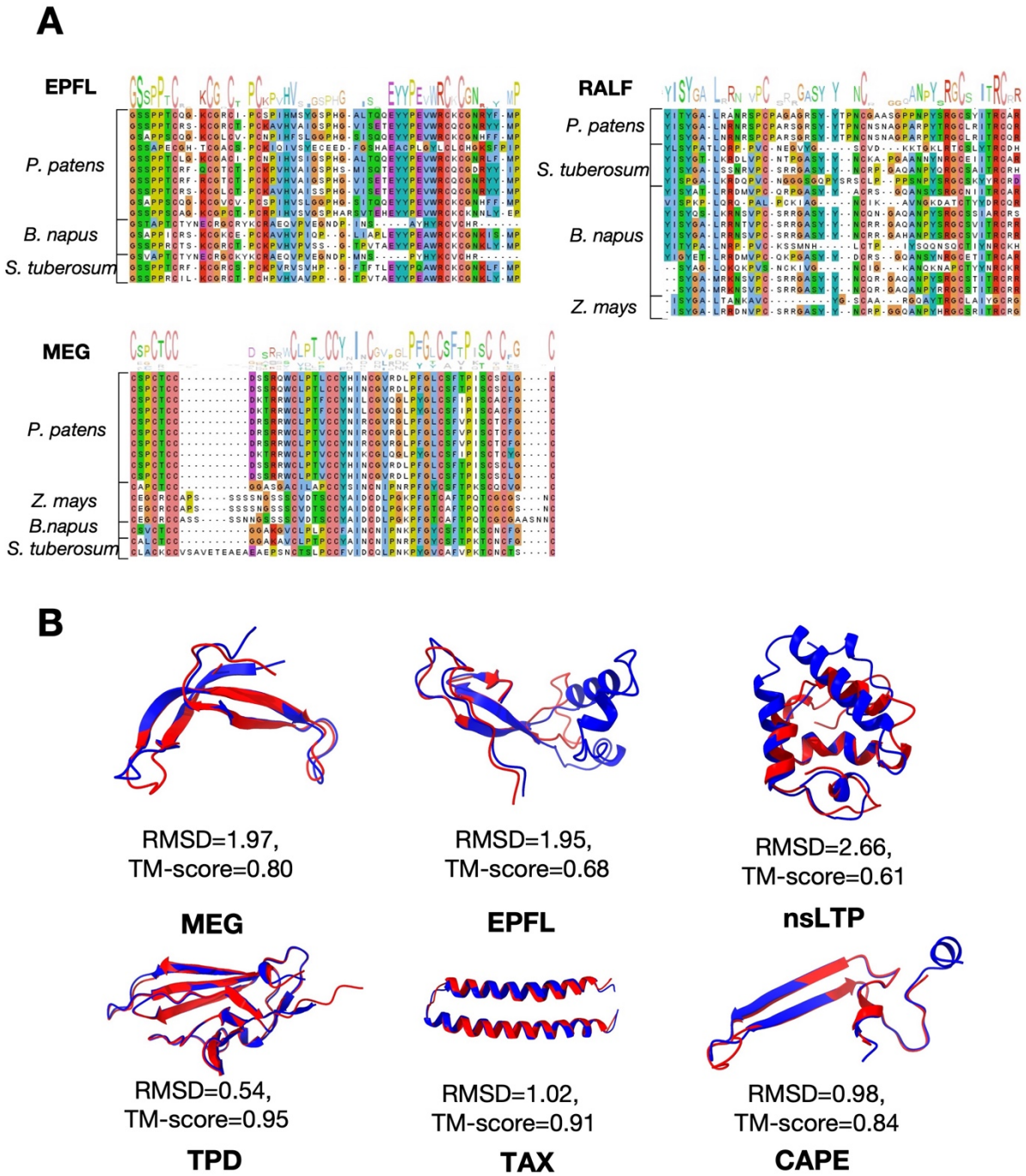

Figure 3. A - Sequence similarity analysis for peptide families in *Physcomitrium patens* and angiosperms; **B -** Structural comparison of angiosperm and *Physcomitrium patens* peptide predicted structures.

Previously, MEG peptides with 8 and 12 cysteine residues were identified in angiosperms (Gutiérrez-Marcos et al., 2004; Slezina et al., 2021). We found that MEG peptides from *P. patens* and *Z. mays*, *S. tuberosum,* and *B. napus* contain 12 conserved cysteine residues,

403 including two CC regions (Figure 3A, Supplementary Figure 2C). In contrast to the cysteine
404 patterns, the MEG peptide sequences showed significant variation among the examined
405 sequences.

406 Thus, our analysis showed that EPFL peptides are the most conserved among all the
407 analyzed plants. The largest difference in peptide motifs was observed in MEG peptides,
408 including the number of cysteine residues and overall amino acid composition.

409

410 Structure-based comparison of the identified SSPs

411 The prediction of peptide structures using AlphaFold2

412 The accuracy of sequence-based methods for predicting peptide structures has been
413 demonstrated in recent years (McDonald et al., 2023). Moreover, current methods for structure
414 comparison allow the detection of distant orthologs (Monzon et al., 2022). Therefore, we next
415 compared structures of EPFL, RALF, CLE, MEG, nsLTP, CAPE, TPD, and TAX peptides
416 from different species. For this, 135 peptide structures were predicted by AlphaFold2 (Jumper
417 et al., 2021), and structures with an average pLDDT > 70 were selected for further analysis.
418 Initially, the peptide structures of *P. patens* were compared with those of angiosperms.
419 Structural alignment was performed using the TM-align tool, and metrics including sequence
420 identity (Seq_Id), Root Mean Square Deviation (RMSD), and TM-score were calculated
421 (Supplementary Table 4). Because clear secondary structures were not predicted for RALF and
422 CLE peptide, they were excluded from further analysis. Overall, 21 peptide structures of MEG,
423 EPFL, CAPE, TPD, TAX, and nsLTP peptides with the highest average pLDDT per family for
424 each plant species were selected for structural comparisons (Supplementary Table 4,
425 Supplementary Materials).

426 The predicted structures of the MEG peptides consist of multiple beta-sheets. The
427 highest similarity to *P. patens* MEG structures was observed in the case of *Z. mays* MEG (TM-
428 score 0.80; Figure 3B) which is in line with our motif comparison. The lowest structural
429 similarity was found between *P. patens* and *S. tuberosum* MEG structures (TM-score 0.44,
430 Supplementary Table 4). The MEG of *Z. mays* contains an additional loop composed of alpha-
431 helices, which is absent in the predicted MEG structure of *P. patens*.

432 The structure of EPFL peptides comprises two anti-parallel beta-sheets connected by a
433 loop. The structures of EPFL peptides from *Z. mays* and *P. patens* showed the highest similarity
434 (TM-score 0.68; Figure 3A) compared to other analyzed plants (TM-scores 0.55 for *B. napus*
435 and *S. tuberosum* (Supplementary Table 4).

436 The predicted structure of non-specific lipid transport proteins (nsLTPs) contains four
437 alpha-helices. *B. napus* nsLTP peptide structure revealed the highest similarity to *P. patens*
438 ndLTP structures (Figure 3B). TM-scores for *Z. mays* and *S. tuberosum* structures compared
439 to *P. patens* were 0.50 and 0.56, respectively (Supplementary Table 4).
440 The predicted structures of the TPD and TAX peptides showed high structural
441 similarity across all examined species (Supplementary Table 4). The highest similarity between
442 the predicted structures of *P. patens* and *B. napus* peptides was observed (Figure 3B).
443 The predicted structures of the CAPE peptides contain two beta-sheets and an alpha-
444 helix. The highest similarity to *P. patens* CAPE was observed between P. *patens* and *B. napus*
445 structures (Figure 3B).
446 Therefore, the cysteine-rich peptides (MEG, EPFL) from *P. patens* showed the highest
447 similarity to *Z. mays* homologs. The structures of CAPE, nsLTP, TAX, and TPD peptides from
448 *P. patens* were the most similar to the predicted structures from *B. napus*. The TPD peptide has
449 the most conserved structure among *P. patens, Z. mays,* and *B. napus* species.

450 The search for structural homologs of identified SSPs

451 Then, we searched for structural homologs of *P. patens* peptide families MEG, EPFL,
452 CAPE, nsLTP, TAX, and TPD against AlphaFold Protein Structure Database
453 (https://alphafold.ebi.ac.uk) and PDB (https://www.rcsb.org) databases by Foldseek (van
454 Kempen et al., 2024).

455 The analysis of MEG peptides yielded three significant hits (TM-score > 0.5,
456 Probability > 0.8) against AlphaFold Database (AFDB) with CRP7-Cysteine-rich family
457 protein from *Zea mays* (Supplementary Figure 3).

458 For EPFL peptides, structural similarity to ~70 EPFL proteins from *Oryza sativa,*
459 *Glycine max, Arabidopsis thaliana, Nicotiana tabacum, etc.* was identified. Hits to structures
460 from the PDB database were also obtained, such as EPFL and plant receptor ERL1-TMM in
461 complex with EPF1 from *Arabidopsis thaliana* (Accessions in PDB database: 2liy_A, 5xkj_F,

462 5xjo_E; Supplementary Figure 3). We also found hits to the structures of nsLTP, TPD, TAX,
463 and CAPE peptides in AlphaFold and PDB databases (Supplementary Figure 3).

464 Thus, our analysis revealed high structural similarity among MEG, EPFL, CAPE,
465 nsLTP, TAX, and TPD peptides from different plant taxonomic groups. For CAPE and EPFL
466 precursors, hits to PDB structures were observed. Therefore, our results confirmed that
467 searches by Foldseek (van Kempen et al., 2024) can be used to find peptide homologs at the
468 structural level.

469 Identification of novel families of SSPs in the moss *P. patens*

470 Novel peptide families have emerged during the evolution of land plants (Furumizu &
471 Shinohara, 2024). However, the identification of taxon-specific peptides and novel peptide
472 families is a challenging task. Moreover, lineage-specific peptide families have been identified
473 only in angiosperms to date. Therefore, we next sought to search for novel SSPs involved in
474 immune response in the non-vascular plant, *P. patens,* using our custom pipeline.

475 At first, we selected 356 ORFs below 200 aa located on DE transcripts that contained a
476 predicted N-terminus signal sequence but did not contain a transmembrane domain or known
477 peptide motif (Figure 1). We additionally filtered out "candidate" SSPs that have protein
478 annotation or have hits in the NCBI non-redundant protein sequence database (BLASTP, E-
479 value < 0.01, organism: *Viridiplantae*). We next searched for possible orthologs of 58
480 "candidate" SSPs in the 1000 plant transcriptome (1KP) database
481 (https://db.cngb.org/datamart/plant/DATApla4/) using TBLASTN (E-value < 0.01). Then, we
482 manually checked the presence of possible peptide motifs based on multiple sequence
483 alignments (MSAs).

484 Based on the analysis of possible paralogs in the *P. patens* genome, we identified two
485 families of putative novel SSPs in *P. patens*. The consensus sequences of identified motifs are
486 presented in Figure 4A (Supplementary figure 4). Family 1 comprises three *P. patens* genes
487 (*Pp3c2_4250*, *Pp3c14_17750*, and *Pp3c21_20040*) that were not functionally annotated yet.
488 One of these genes, *Pp3c21_20040*, was differentially regulated upon *B. cinerea* infection
489 (Figure 4A, Supplementary figure 4A). The members of Family 1 are cysteine-rich and
490 comprise 8 conservative cysteine residues as well as conserved "NATH" and "SCGF" motifs
491 (Figure 4A). The TBLASTN search in the 1KP database identified possible orthologs in 49

species, including mosses, liverworts, and lycophytes (Figure 4A, Supplementary Figure 5). The median length of predicted ORFs was 119 aa.

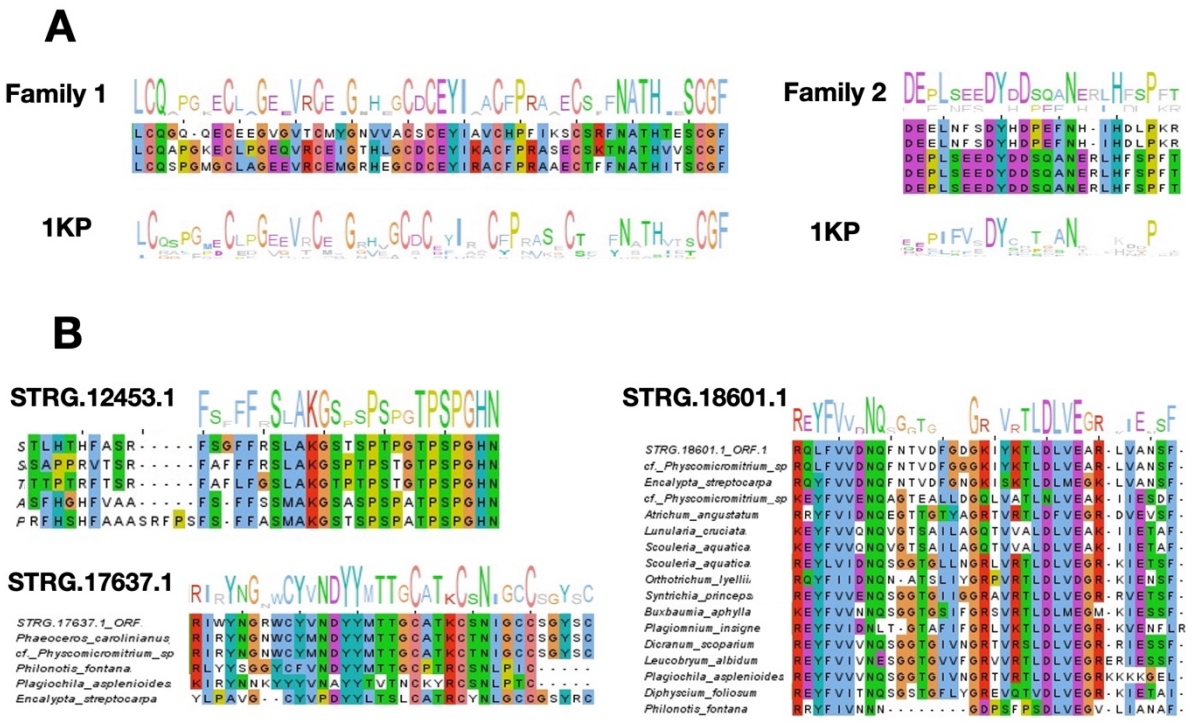

Figure 4. **A -** Alignment logos of novel candidate families found in *P. patens* (**Family 1:** STRG.19963.1_ORF.1; STRG.1695.1_ORF.2; STRG.14124.1_ORF.4; alignment logo with 1KP; **Family 2:** STRG.4116.1_ORF.1; STRG.4116.2_ORF.1; STRG.4476.2_ORF.1; STRG.4476.3_ORF.1; STRG.4473.1_ORF.1; alignment logo with 1KP); **B -** Alignment logos of novel peptide candidates corresponding to unique *P. patens* ORFs with 1KP (STRG.12453.1_ORF.5; STRG.18601.1_ORF.1; STRG.17637.1_ORF.1).

The putative peptide precursors of Family 2 shared two similar peptide motifs: DY*D***N**H**P and DY*D***N***H**P (Figure 4A, Supplementary Figure 4B). These motifs are similar to the known PSY peptide motif DY*(D)(P)**N**H*P (Furumizu et al., 2021), but differ in the position of conserved residues H and P. Previously, one *P. patens* gene (Pp3c8_3200) was identified as a precursor of PSY peptide (Furumizu et al., 2021; Tost et al., 2021). Two predicted protein precursors from Family 2, STRG.4116.1_ORF.1 (117 aa) and STRG.4116.2_ORF.1 (91aa), shared the DY*D***N**H**P motif at the C-end and came from the *Pp3c3_33940V3.3* gene that was erroneously annotated as alternative splicing factor SRp20/9G8 in Phytozome 13. The STRG.4116.1 transcript was differentially up-regulated upon infection with *B. cinerea*. The other three predicted precursors contain the motif

511 DY*D***N***H**P. Two of them, STRG.4476.2_ORF.1 (114 aa) and STRG.4476.3_ORF.1
512 (118 aa) belonged to the gene *Pp3c4_6140*. The assembled transcript STRG.4473.1 intersects
513 the *P. patens* gene *Pp3c4_6040* and encodes 118 aa precursor STRG.4473.1_ORF.1. Thus, we
514 identified a novel family of PSY-like peptides that are encoded by three *P. patens* loci. The
515 TBLASTN analysis against 1000 Plant transcriptomes identified 20 possible orthologs of
516 Family 2 in mosses and one liverwort species (Supplementary Figure 6). The median length of
517 predicted ORFs was 110 aa which is similar to known PSY genes.

518 Because SSP can be presented by only one copy in the genomes of non-vascular plants,
519 we additionally analyzed putative SSP precursors without possible paralogs in *P. patens*. We
520 searched for their possible homologs against transcripts from 1KP database. The resulting
521 alignments of three most interesting up-regulated peptide candidates are presented in Figure
522 4B. Full alignments can be found in Supplementary Figure 7. These putative peptide precursors
523 contain motifs that are conserved among different plant species. In the case of
524 STRG.12453.1_ORF.5 (140aa), P***TPSPGHN motif is observed, which similar to CLE and
525 IDA peptide motifs (Furumizu et al., 2021). This candidate was found in four moss species
526 (Figure 4B, Supplementary Figure 7A). Candidate STRG.18601.1_ORF.1 (115aa) contains a
527 conserved LDLVE motif, which is observed in 13 other species, including mosses and
528 liverworts (Figure 4A, Supplementary Figure 7B). Finally, *P. patens* candidate
529 STRG.17637.1_ORF.1 (121aa) is cysteine-rich and, notably, it contains a conserved DYY
530 region. Hits to four other species were found, including moss, liverwort, and hornwort plants
531 (Figure 4B, Supplementary Figure 7C).

532 Thus, we propose an approach to identify novel, not annotated, plant peptide families. This
533 approach focuses on motif analysis of ORFs from DE transcripts, both with the presence of
534 SSP features (proper length, N-terminal signal sequence, no TM-domain) and the absence of
535 annotated protein domains, homology to known proteins. We identified 5 potential candidates
536 for novel signaling peptides in *P. patens*. Two of them comprise families based on sequence
537 similarity, and some of them are unique ORFs predicted in *P. patens.* Nevertheless, all potential
538 novel candidates are found in other plant species belonging to non-vascular plants. For two
539 candidates, distant homology to known peptide families (PSY, IDA, and CLE) is suspected.

540

541 # Discussion

542 Recent studies showed that peptides derived from protein precursors play an important
543 role in plant immunity, modulating the defense response. The plant cell-surface receptors that
544 recognize these peptide ligands contain Leucine-Rich Repeat (LRR) or Malectin ectodomains
545 and have an ancient origin (Ngou et al., 2024). Contrary to immune receptors, the origin and
546 evolution of immune peptides are still poorly understood (Furumizu et al., 2021). One of the
547 reasons is that, due to rapid changes, they appear to quickly enter the "twilight zone", where
548 sequence similarity is no longer detectable. Nevertheless, the several databases that include
549 plant Small Secreted Peptides (SSPs) were recently published (Boschiero et al., 2020; Ghorbani
550 et al., 2015; Pan et al., 2013). Sequence similarity, however, does not necessarily mean
551 functional similarity across different plant phyla. In this study, we compared pathogen-induced
552 transcriptomes in vascular and non-vascular plants to understand how SSP families from
553 different plant lineages respond to infection. Along with conserved SSPs associated with
554 immune responses that were found in the transcriptomes of both vascular and non-vascular
555 plants, we observed species-specific regulation of certain SSP families.

556 Our analysis shows that cysteine-rich peptides were actively regulated during infection
557 in all plant lineages. The EPFL, RALF, TAX, and MEG were differentially regulated in *P.*
558 *patens* and angiosperm species. The widely conserved family of EPIDERMAL PATTERNING
559 FACTOR (EPF) peptides is involved in regulating plant growth or development in vascular
560 and non-vascular land plants (Caine et al., 2016; Y. He et al., 2023). The nine EPFL genes that
561 are upregulated in the developing sporophyte have been identified in previous bioinformatics
562 studies of the *P. patens* genome (Caine et al., 2016; Lyapina et al., 2021; Takata et al., 2013),
563 but their functions remain unknown. However, the role of EPF and EPF-LIKE (EPFL) peptides
564 as positive or negative regulators of immune response has not been shown to date.
565 Nevertheless, several genes of the EPFL family were shown to be significantly down-regulated
566 upon pathogen infection in tomato (Slezina et al., 2021). In this study, we found that the
567 transcriptional level of six EPFL genes was significantly down-regulated in *P. patens*. This
568 result can be explained by a specific response to pathogens or by the inhibition of growth
569 processes under stress conditions.

570 Our treatment of moss protonemata with synthetic EPFL peptide resulted in an increase
571 in intracellular reactive oxygen species (ROS) levels, suggesting the activation of downstream

572 signaling. In Arabidopsis, the receptor-like kinase (RLK) ERECTA and its two closely related
573 homologs, ERECTA-LIKE 1 (ERL1) and ERL2 are responsible for perceiving the EPF/EPFL
574 family peptides (Y. He et al., 2023; Tameshige et al., 2017). In the genome of *P. patens,* six
575 potential orthologues of the ERECTA genes were found (Villagarcia et al., 2012). Thus, the
576 EPFL family might be a target for future work on understanding the evolution of
577 phytocytokines in land plants.

578 The RALF peptides were shown to be involved in immune response across different
579 plant lineages (Y.-H. He et al., 2023; Mamaeva et al., 2023; Slezina et al., 2021; Wolf & Höfte,
580 2014). We found both up-regulated and down-regulated RALF genes in pathogen-induced
581 transcriptomes, which is consistent with previous results showing different roles of different
582 members of RALFs in modulating plant immunity (Y.-H. He et al., 2023; L. Liu et al., 2024;
583 Mamaeva et al., 2023; Stegmann et al., 2017).

584 The poorly characterized cysteine-rich peptides, such as TAX and MEG were
585 differentially regulated in both vascular and non-vascular plant species. However, how TAX
586 peptides are involved in immune response is currently unknown. Previously, the tomato MEGs
587 were found to be down-regulated in response to infection (Slezina et al., 2021). This is similar
588 to our findings and suggests the conservative role of this SSP family in vascular and non-
589 vascular land plants. Nevertheless, the role of MEG peptides in plant growth and defense is
590 poorly understood.

591 In addition to common approaches for the identification of SSPs based on sequence
592 similarity (Boschiero et al., 2020), we developed a new pipeline to identify novel lineage-
593 specific secreted peptides. Our pipeline resulted in the identification of two putative SSP
594 families in *P. patens*. One of these families (Family 2) consists of PSY-like peptides, which
595 are similar to the known phytocytokine PSY family in angiosperms. The PSY peptide family
596 was present in the most recent common ancestor of vascular plants and bryophytes (Furumizu
597 & Shinohara, 2024). Previously, one gene potentially encoding the PSY peptide and another
598 encoding the cognate PSYR receptor were identified in *P. patens* (Furumizu et al., 2021;
599 Furumizu & Aalen, 2023). Thus, we significantly expand the family of PSY-like peptides in
600 bryophytes. The identification of previously unknown PSY-like peptides in bryophyte genomes
601 could expand our understanding of the peptide evolution in land plants.

602 In conclusion, our comprehensive analysis of small secreted peptides in the pathogen-
603 induced transcriptomes of four plant species showed the conservation of cysteine-rich peptides
604 across different plant lineages. We found high motif and structural conservation of these
605 peptides in vascular and non-vascular plants. In addition, we identified previously
606 uncharacterized putative SSP families in bryophytes. One of these bryophyte-specific families
607 shows similarity to previously characterized PSY peptides. Thus, our study provides a new
608 avenue to explore the evolution of known and previously uncharacterized peptide families.

609 Author contributions

610 IF supervised the study. IL, DG conducted all experiments and performed all bioinformatic
611 analyses. AM performed ROS measurement. EAR, DYR and EVR synthesized recombinant
612 moss *P. patens* peptides. IL, DG and IF wrote the manuscript. All authors contributed to the
613 article and approved the submitted version.

614 Funding

615 This work was supported by Russian Science Foundation (project no. 23-74-10048).

616 Data availability statement

617 The data that support the findings were derived from the NCBI Sequence Reads Archive (SRA)
618 available in the public domain with following accession numbers: SRP274010, SRP390856,
619 SRP053361, SRP066006.

620 **References**

621 Andrews, S. (2010). *FastQC: A Quality Control tool for High Throughput Sequence Data*.
622 https://www.bioinformatics.babraham.ac.uk/projects/fastqc/

623 Bolger, A. M., Lohse, M., & Usadel, B. (2014). Trimmomatic: A flexible trimmer for Illumina
624 sequence data. *Bioinformatics (Oxford, England)*, *30*(15), 2114–2120.
625 https://doi.org/10.1093/bioinformatics/btu170

626 Boschiero, C., Dai, X., Lundquist, P. K., Roy, S., Bang, T. C. de, Zhang, S., Zhuang, Z., Torres-

Jerez, I., Udvardi, M. K., Scheible, W.-R., & Zhao, P. X. (2020). MtSSPdb: The Medicago truncatula Small Secreted Peptide Database. *Plant Physiology*, *183*(1), 399–413. https://doi.org/10.1104/pp.19.01088

Bowman, J. L. (2022). The origin of a land flora. *Nature Plants*, *8*(12), 1352–1369. https://doi.org/10.1038/s41477-022-01283-y

Bowman, J. L., Kohchi, T., Yamato, K. T., Jenkins, J., Shu, S., Ishizaki, K., Yamaoka, S., Nishihama, R., Nakamura, Y., Berger, F., Adam, C., Aki, S. S., Althoff, F., Araki, T., Arteaga-Vazquez, M. A., Balasubrmanian, S., Barry, K., Bauer, D., Boehm, C. R., … Schmutz, J. (2017). Insights into Land Plant Evolution Garnered from the Marchantia polymorpha Genome. *Cell*, *171*(2), 287-304.e15. https://doi.org/10.1016/j.cell.2017.09.030

Caine, R. S., Chater, C. C., Kamisugi, Y., Cuming, A. C., Beerling, D. J., Gray, J. E., & Fleming, A. J. (2016). An ancestral stomatal patterning module revealed in the non-vascular land plant Physcomitrella patens. *Development*, *143*(18), 3306–3314. https://doi.org/10.1242/dev.135038

de Bang, T. C., Lay, K. S., Scheible, W.-R., & Takahashi, H. (2017). Small peptide signaling pathways modulating macronutrient utilization in plants. *Current Opinion in Plant Biology*, *39*, 31–39. https://doi.org/10.1016/j.pbi.2017.05.005

Fesenko, I., Shabalina, S. A., Mamaeva, A., Knyazev, A., Glushkevich, A., Lyapina, I., Ziganshin, R., Kovalchuk, S., Kharlampieva, D., Lazarev, V., Taliansky, M., & Koonin, E. V. (2021). A vast pool of lineage-specific microproteins encoded by long non-coding RNAs in plants. *Nucleic Acids Research*, *49*(18), 10328–10346. https://doi.org/10.1093/nar/gkab816

Furumizu, C., & Aalen, R. B. (2023). Peptide signaling through leucine-rich repeat receptor kinases: Insight into land plant evolution. *New Phytologist*, *238*(3), 977–982. https://doi.org/10.1111/nph.18827

Furumizu, C., Krabberød, A. K., Hammerstad, M., Alling, R. M., Wildhagen, M., Sawa, S., & Aalen, R. B. (2021). The sequenced genomes of nonflowering land plants reveal the innovative evolutionary history of peptide signaling. *The Plant Cell*, *33*(9), 2915–2934. https://doi.org/10.1093/plcell/koab173

Furumizu, C., & Shinohara, H. (2024). Land plant peptide signaling: What we know—and don't know—about its evolution. *Physiologia Plantarum*, *176*(1), e14172. https://doi.org/10.1111/ppl.14172

Ghorbani, S., Lin, Y.-C., Parizot, B., Fernandez, A., Njo, M. F., Van de Peer, Y., Beeckman, T., & Hilson, P. (2015). Expanding the repertoire of secretory peptides controlling root development with comparative genome analysis and functional assays. *Journal of Experimental Botany*, *66*(17), 5257–5269. https://doi.org/10.1093/jxb/erv346

Goodstein, D. M., Shu, S., Howson, R., Neupane, R., Hayes, R. D., Fazo, J., Mitros, T., Dirks, W., Hellsten, U., Putnam, N., & Rokhsar, D. S. (2012). Phytozome: A comparative platform for green plant genomics. *Nucleic Acids Research*, *40*(Database issue), D1178-1186. https://doi.org/10.1093/nar/gkr944

Gutiérrez-Marcos, J. F., Costa, L. M., Biderre-Petit, C., Khbaya, B., O'Sullivan, D. M.,

Wormald, M., Perez, P., & Dickinson, H. G. (2004). Maternally expressed gene1 Is a novel maize endosperm transfer cell-specific gene with a maternal parent-of-origin pattern of expression. *The Plant Cell*, *16*(5), 1288–1301. https://doi.org/10.1105/tpc.019778

Hanada, K., Higuchi-Takeuchi, M., Okamoto, M., Yoshizumi, T., Shimizu, M., Nakaminami, K., Nishi, R., Ohashi, C., Iida, K., Tanaka, M., Horii, Y., Kawashima, M., Matsui, K., Toyoda, T., Shinozaki, K., Seki, M., & Matsui, M. (2013). Small open reading frames associated with morphogenesis are hidden in plant genomes. *Proceedings of the National Academy of Sciences*, *110*(6), 2395–2400. https://doi.org/10.1073/pnas.1213958110

He, Y., He, X., Wang, X., Hao, M., Gao, J., Wang, Y., Yang, Z.-N., & Meng, X. (2023). An EPFL peptide signaling pathway promotes stamen elongation via enhancing filament cell proliferation to ensure successful self-pollination in Arabidopsis thaliana. *New Phytologist*, *238*(3), 1045–1058. https://doi.org/10.1111/nph.18806

He, Y.-H., Chen, S.-Y., Chen, X.-Y., Xu, Y.-P., Liang, Y., & Cai, X.-Z. (2023). RALF22 promotes plant immunity and amplifies the Pep3 immune signal. *Journal of Integrative Plant Biology*, *65*(11), 2519–2534. https://doi.org/10.1111/jipb.13566

Hou, S., Liu, D., & He, P. (2021). Phytocytokines function as immunological modulators of plant immunity. *Stress Biology*, *1*(1), 8. https://doi.org/10.1007/s44154-021-00009-y

Hsu, P. Y., & Benfey, P. N. (2018). Small but Mighty: Functional Peptides Encoded by Small ORFs in Plants. *PROTEOMICS*, *18*(10), 1700038. https://doi.org/10.1002/pmic.201700038

Hu, X.-L., Lu, H., Hassan, M. M., Zhang, J., Yuan, G., Abraham, P. E., Shrestha, H. K., Villalobos Solis, M. I., Chen, J.-G., Tschaplinski, T. J., Doktycz, M. J., Tuskan, G. A., Cheng, Z.-M. (Max), & Yang, X. (2021). Advances and perspectives in discovery and functional analysis of small secreted proteins in plants. *Horticulture Research*, *8*(1), 1–14. https://doi.org/10.1038/s41438-021-00570-7

Huang, J., Zhang, T., Linstroth, L., Tillman, Z., Otegui, M. S., Owen, H. A., & Zhao, D. (2016). Control of Anther Cell Differentiation by the Small Protein Ligand TPD1 and Its Receptor EMS1 in Arabidopsis. *PLOS Genetics*, *12*(8), e1006147. https://doi.org/10.1371/journal.pgen.1006147

Jumper, J., Evans, R., Pritzel, A., Green, T., Figurnov, M., Ronneberger, O., Tunyasuvunakool, K., Bates, R., Žídek, A., Potapenko, A., Bridgland, A., Meyer, C., Kohl, S. A. A., Ballard, A. J., Cowie, A., Romera-Paredes, B., Nikolov, S., Jain, R., Adler, J., … Hassabis, D. (2021). Highly accurate protein structure prediction with AlphaFold. *Nature*, *596*(7873), 583–589. https://doi.org/10.1038/s41586-021-03819-2

Katoh, K., & Standley, D. M. (2013). MAFFT Multiple Sequence Alignment Software Version 7: Improvements in Performance and Usability. *Molecular Biology and Evolution*, *30*(4), 772–780. https://doi.org/10.1093/molbev/mst010

Kim, D., Langmead, B., & Salzberg, S. L. (2015). HISAT: A fast spliced aligner with low memory requirements. *Nature Methods*, *12*(4), 357–360. https://doi.org/10.1038/nmeth.3317

Kulaeva, O., Kliukova, M., Afonin, A., Sulima, A., Zhukov, V., & Tikhonovich, I. (2020). The role of plant antimicrobial peptides (AMPs) in response to biotic and abiotic environmental

factors. *Biological Communications*, *65*(2), Article 2. https://doi.org/10.21638/spbu03.2020.205

Kwenda, S., Birch, P. R. J., & Moleleki, L. N. (2016). Genome-wide identification of potato long intergenic noncoding RNAs responsive to Pectobacterium carotovorum subspecies brasiliense infection. *BMC Genomics*, *17*(1), 614. https://doi.org/10.1186/s12864-016-2967-9

Li, H., Handsaker, B., Wysoker, A., Fennell, T., Ruan, J., Homer, N., Marth, G., Abecasis, G., Durbin, R., & 1000 Genome Project Data Processing Subgroup. (2009). The Sequence Alignment/Map format and SAMtools. *Bioinformatics (Oxford, England)*, *25*(16), 2078–2079. https://doi.org/10.1093/bioinformatics/btp352

Li, Y., Di, Q., Luo, L., & Yu, L. (2024). Phytosulfokine peptides, their receptors, and functions. *Frontiers in Plant Science*, *14*. https://doi.org/10.3389/fpls.2023.1326964

Lima, A. M., Azevedo, M. I. G., Sousa, L. M., Oliveira, N. S., Andrade, C. R., Freitas, C. D. T., & Souza, P. F. N. (2022). Plant antimicrobial peptides: An overview about classification, toxicity and clinical applications. *International Journal of Biological Macromolecules*, *214*, 10–21. https://doi.org/10.1016/j.ijbiomac.2022.06.043

Liu, L., Liu, X., Bai, Z., Tanveer, M., Zhang, Y., Chen, W., Shabala, S., & Huang, L. (2024). Small but powerful: RALF peptides in plant adaptive and developmental responses. *Plant Science*, *343*, 112085. https://doi.org/10.1016/j.plantsci.2024.112085

Liu, Z., Hou, S., Rodrigues, O., Wang, P., Luo, D., Munemasa, S., Lei, J., Liu, J., Ortiz-Morea, F. A., Wang, X., Nomura, K., Yin, C., Wang, H., Zhang, W., Zhu-Salzman, K., He, S. Y., He, P., & Shan, L. (2022). Phytocytokine signalling reopens stomata in plant immunity and water loss. *Nature*, *605*(7909), 332–339. https://doi.org/10.1038/s41586-022-04684-3

Lori, M., van Verk, M. C., Hander, T., Schatowitz, H., Klauser, D., Flury, P., Gehring, C. A., Boller, T., & Bartels, S. (2015). Evolutionary divergence of the plant elicitor peptides (Peps) and their receptors: Interfamily incompatibility of perception but compatibility of downstream signalling. *Journal of Experimental Botany*, *66*(17), 5315–5325. https://doi.org/10.1093/jxb/erv236

Lyapina, I., Filippova, A., & Fesenko, I. (2019). The Role of Peptide Signals Hidden in the Structure of Functional Proteins in Plant Immune Responses. *International Journal of Molecular Sciences*, *20*(18), 4343. https://doi.org/10.3390/ijms20184343

Lyapina, I., Filippova, A., Kovalchuk, S., Ziganshin, R., Mamaeva, A., Lazarev, V., Latsis, I., Mikhalchik, E., Panasenko, O., Ivanov, O., Ivanov, V., & Fesenko, I. (2021). Possible role of small secreted peptides (SSPs) in immune signaling in bryophytes. *Plant Molecular Biology*, *106*(1–2), 123–143. https://doi.org/10.1007/s11103-021-01133-z

Mamaeva, A., Lyapina, I., Knyazev, A., Golub, N., Mollaev, T., Chudinova, E., Elansky, S., Babenko, V. V., Veselovsky, V. A., Klimina, K. M., Gribova, T., Kharlampieva, D., Lazarev, V., & Fesenko, I. (2023). RALF peptides modulate immune response in the moss Physcomitrium patens. *Frontiers in Plant Science*, *14*. https://doi.org/10.3389/fpls.2023.1077301

McDonald, E. F., Jones, T., Plate, L., Meiler, J., & Gulsevin, A. (2023). Benchmarking

AlphaFold2 on Peptide Structure Prediction. *Structure (London, England : 1993)*, *31*(1), 111-119.e2. https://doi.org/10.1016/j.str.2022.11.012

Monzon, V., Paysan-Lafosse, T., Wood, V., & Bateman, A. (2022). Reciprocal best structure hits: Using AlphaFold models to discover distant homologues. *Bioinformatics Advances*, *2*(1), vbac072. https://doi.org/10.1093/bioadv/vbac072

Moravej, H., Moravej, Z., Yazdanparast, M., Heiat, M., Mirhosseini, A., Moosazadeh Moghaddam, M., & Mirnejad, R. (2018). Antimicrobial Peptides: Features, Action, and Their Resistance Mechanisms in Bacteria. *Microbial Drug Resistance*, *24*(6), 747–767. https://doi.org/10.1089/mdr.2017.0392

Ngou, B. P. M., Wyler, M., Schmid, M. W., Kadota, Y., & Shirasu, K. (2024). Evolutionary trajectory of pattern recognition receptors in plants. *Nature Communications*, *15*(1), 308. https://doi.org/10.1038/s41467-023-44408-3

Ogawa-Ohnishi, M., Yamashita, T., Kakita, M., Nakayama, T., Ohkubo, Y., Hayashi, Y., Yamashita, Y., Nomura, T., Noda, S., Shinohara, H., & Matsubayashi, Y. (2022). Peptide ligand-mediated trade-off between plant growth and stress response. *Science (New York, N.Y.)*, *378*(6616), 175–180. https://doi.org/10.1126/science.abq5735

Olsson, V., Joos, L., Zhu, S., Gevaert, K., Butenko, M. A., & De Smet, I. (2019). Look Closely, the Beautiful May Be Small: Precursor-Derived Peptides in Plants. *Annual Review of Plant Biology*, *70*, 153–186. https://doi.org/10.1146/annurev-arplant-042817-040413

Pan, B., Sheng, J., Sun, W., Zhao, Y., Hao, P., & Li, X. (2013). OrysPSSP: A comparative Platform for Small Secreted Proteins from rice and other plants. *Nucleic Acids Research*, *41*(D1), D1192–D1198. https://doi.org/10.1093/nar/gks1090

Pertea, M., Pertea, G. M., Antonescu, C. M., Chang, T.-C., Mendell, J. T., & Salzberg, S. L. (2015). StringTie enables improved reconstruction of a transcriptome from RNA-seq reads. *Nature Biotechnology*, *33*(3), 290–295. https://doi.org/10.1038/nbt.3122

Quevillon, E., Silventoinen, V., Pillai, S., Harte, N., Mulder, N., Apweiler, R., & Lopez, R. (2005). InterProScan: Protein domains identifier. *Nucleic Acids Research*, *33*(Web Server issue), W116–W120. https://doi.org/10.1093/nar/gki442

Reboledo, G., Agorio, A. D., Vignale, L., Batista-García, R. A., & Ponce De León, I. (2021). Transcriptional profiling reveals conserved and species-specific plant defense responses during the interaction of Physcomitrium patens with Botrytis cinerea. *Plant Molecular Biology*, *107*(4–5), 365–385. https://doi.org/10.1007/s11103-021-01116-0

Rhodes, J., Roman, A.-O., Bjornson, M., Brandt, B., Derbyshire, P., Wyler, M., Schmid, M. W., Menke, F. L., Santiago, J., & Zipfel, C. (2022). Perception of a conserved family of plant signalling peptides by the receptor kinase HSL3. *eLife*, *11*, e74687. https://doi.org/10.7554/eLife.74687

Robinson, M. D., McCarthy, D. J., & Smyth, G. K. (2010). edgeR: A Bioconductor package for differential expression analysis of digital gene expression data. *Bioinformatics (Oxford, England)*, *26*(1), 139–140. https://doi.org/10.1093/bioinformatics/btp616

786 Ryan, C. A., & Pearce, G. (2003). Systemins: A functionally defined family of peptide signals
787 that regulate defensive genes in Solanaceae species. *Proceedings of the National Academy of*
788 *Sciences*, *100*(suppl_2), 14577–14580. https://doi.org/10.1073/pnas.1934788100

789 Rzemieniewski, J., & Stegmann, M. (2022). Regulation of pattern-triggered immunity and
790 growth by phytocytokines. *Current Opinion in Plant Biology*, *68*, 102230.
791 https://doi.org/10.1016/j.pbi.2022.102230

792 Santos-Silva, C. A. dos, Ferreira-Neto, J. R. C., Amador, V. C., Bezerra-Neto, J. P., Vilela, L.
793 M. B., Binneck, E., Rêgo, M. de S., da Silva, M. D., Mangueira de Melo, A. L. T., da Silva, R.
794 H., & Benko-Iseppon, A. M. (2023). From Gene to Transcript and Peptide: A Deep Overview
795 on Non-Specific Lipid Transfer Proteins (nsLTPs). *Antibiotics*, *12*(5), Article 5.
796 https://doi.org/10.3390/antibiotics12050939

797 Shevchuk, N. A., Bryksin, A. V., Nusinovich, Y. A., Cabello, F. C., Sutherland, M., & Ladisch,
798 S. (2004). Construction of long DNA molecules using long PCR-based fusion of several
799 fragments simultaneously. *Nucleic Acids Research*, *32*(2), e19.
800 https://doi.org/10.1093/nar/gnh014

801 Singh, U., & Wurtele, E. S. (2021). orfipy: A fast and flexible tool for extracting ORFs.
802 *Bioinformatics*, *37*(18), 3019–3020. https://doi.org/10.1093/bioinformatics/btab090

803 Slezina, M. P., Istomina, E. A., Korostyleva, T. V., Kovtun, A. S., Kasianov, A. S., Konopkin,
804 A. A., Shcherbakova, L. A., & Odintsova, T. I. (2021). Molecular Insights into the Role of
805 Cysteine-Rich Peptides in Induced Resistance to Fusarium oxysporum Infection in Tomato
806 Based on Transcriptome Profiling. *International Journal of Molecular Sciences*, *22*(11), 5741.
807 https://doi.org/10.3390/ijms22115741

808 Stegmann, M., Monaghan, J., Smakowska-Luzan, E., Rovenich, H., Lehner, A., Holton, N.,
809 Belkhadir, Y., & Zipfel, C. (2017). The receptor kinase FER is a RALF-regulated scaffold
810 controlling plant immune signaling. *Science*, *355*(6322), 287–289.
811 https://doi.org/10.1126/science.aal2541

812 Takata, N., Yokota, K., Ohki, S., Mori, M., Taniguchi, T., & Kurita, M. (2013). Evolutionary
813 Relationship and Structural Characterization of the EPF/EPFL Gene Family. *PLOS ONE*, *8*(6),
814 e65183. https://doi.org/10.1371/journal.pone.0065183

815 Tam, J. P., Wang, S., Wong, K. H., & Tan, W. L. (2015). Antimicrobial Peptides from Plants.
816 *Pharmaceuticals*, *8*(4), 711–757. https://doi.org/10.3390/ph8040711

817 Tameshige, T., Ikematsu, S., Torii, K. U., & Uchida, N. (2017). Stem development through
818 vascular tissues: EPFL-ERECTA family signaling that bounces in and out of phloem. *Journal*
819 *of Experimental Botany*, *68*(1), 45–53. https://doi.org/10.1093/jxb/erw447

820 Tanaka, K., & Heil, M. (2021). Damage-Associated Molecular Patterns (DAMPs) in Plant
821 Innate Immunity: Applying the Danger Model and Evolutionary Perspectives. *Annual Review*
822 *of Phytopathology*, *59*(Volume 59, 2021), 53–75. https://doi.org/10.1146/annurev-phyto-
823 082718-100146

824 Tavormina, P., De Coninck, B., Nikonorova, N., De Smet, I., & Cammue, B. P. A. (2015). The
825 Plant Peptidome: An Expanding Repertoire of Structural Features and Biological Functions.

The Plant Cell, *27*(8), 2095–2118. https://doi.org/10.1105/tpc.15.00440

Tian, D., Xie, Q., Deng, Z., Xue, J., Li, W., Zhang, Z., Dai, Y., Zheng, B., Lu, T., De Smet, I., & Guo, Y. (2022). Small secreted peptides encoded on the wheat (triticum aestivum L.) genome and their potential roles in stress responses. *Frontiers in Plant Science*, *13*, 1000297. https://doi.org/10.3389/fpls.2022.1000297

Tost, A. S., Kristensen, A., Olsen, L. I., Axelsen, K. B., & Fuglsang, A. T. (2021). The PSY Peptide Family—Expression, Modification and Physiological Implications. *Genes*, *12*(2), Article 2. https://doi.org/10.3390/genes12020218

van Kempen, M., Kim, S. S., Tumescheit, C., Mirdita, M., Lee, J., Gilchrist, C. L. M., Söding, J., & Steinegger, M. (2024). Fast and accurate protein structure search with Foldseek. *Nature Biotechnology*, *42*(2), 243–246. https://doi.org/10.1038/s41587-023-01773-0

Villagarcia, H., Morin, A.-C., Shpak, E. D., & Khodakovskaya, M. V. (2012). Modification of tomato growth by expression of truncated ERECTA protein from Arabidopsis thaliana. *Journal of Experimental Botany*, *63*(18), 6493–6504. https://doi.org/10.1093/jxb/ers305

Wang, D., Jin, S., Chen, Z., Shan, Y., & Li, L. (2022). Genome-wide identification of the pectin methylesterase inhibitor genes in Brassica napus and expression analysis of selected members. *Frontiers in Plant Science*, *13*, 940284. https://doi.org/10.3389/fpls.2022.940284

Wang, P., Yao, S., Kosami, K., Guo, T., Li, J., Zhang, Y., Fukao, Y., Kaneko-Kawano, T., Zhang, H., She, Y.-M., Wang, P., Xing, W., Hanada, K., Liu, R., & Kawano, Y. (2020). Identification of endogenous small peptides involved in rice immunity through transcriptomics- and proteomics-based screening. *Plant Biotechnology Journal*, *18*(2), 415–428. https://doi.org/10.1111/pbi.13208

Waterhouse, A. M., Procter, J. B., Martin, D. M. A., Clamp, M., & Barton, G. J. (2009). Jalview Version 2—A multiple sequence alignment editor and analysis workbench. *Bioinformatics*, *25*(9), 1189–1191. https://doi.org/10.1093/bioinformatics/btp033

Wolf, S., & Höfte, H. (2014). Growth Control: A Saga of Cell Walls, ROS, and Peptide Receptors. *The Plant Cell*, *26*(5), 1848–1856. https://doi.org/10.1105/tpc.114.125518

Xia, X., Wei, Q., Xiao, C., Ye, Y., Li, Z., Marivingt-Mounir, C., Chollet, J.-F., Liu, W., & Wu, H. (2023). Genomic survey of NPF and NRT2 transporter gene families in five inbred maize lines and their responses to pathogens infection. *Genomics*, *115*(2), 110555. https://doi.org/10.1016/j.ygeno.2022.110555

Xiong, L., Huang, Y., Liu, Z., Li, C., Yu, H., Shahid, M. Q., Lin, Y., Qiao, X., Xiao, J., Gray, J. E., & Jin, J. (2022). Small EPIDERMAL PATTERNING FACTOR-LIKE2 peptides regulate awn development in rice. *Plant Physiology*, *190*(1), 516–531. https://doi.org/10.1093/plphys/kiac278

Yang, H., Kim, X., Skłenar, J., Aubourg, S., Sancho-Andrés, G., Stahl, E., Guillou, M.-C., Gigli-Bisceglia, N., Tran Van Canh, L., Bender, K. W., Stintzi, A., Reymond, P., Sánchez-Rodríguez, C., Testerink, C., Renou, J.-P., Menke, F. L. H., Schaller, A., Rhodes, J., & Zipfel, C. (2023). Subtilase-mediated biogenesis of the expanded family of SERINE RICH ENDOGENOUS PEPTIDES. *Nature Plants*, *9*(12), 2085–2094.

https://doi.org/10.1038/s41477-023-01583-x

Zhang, J.-M., & An, J. (2007). Cytokines, inflammation, and pain. *International Anesthesiology Clinics*, *45*(2), 27–37. https://doi.org/10.1097/AIA.0b013e318034194e

Zhang, R., Shi, P.-T., Zhou, M., Liu, H.-Z., Xu, X.-J., Liu, W.-T., & Chen, K.-M. (2023). Rapid alkalinization factor: Function, regulation, and potential applications in agriculture. *Stress Biology*, *3*(1), 16. https://doi.org/10.1007/s44154-023-00093-2

Zhang, Y., & Skolnick, J. (2005). TM-align: A protein structure alignment algorithm based on the TM-score. *Nucleic Acids Research*, *33*(7), 2302–2309. https://doi.org/10.1093/nar/gki524

Ziemann, S., van der Linde, K., Lahrmann, U., Acar, B., Kaschani, F., Colby, T., Kaiser, M., Ding, Y., Schmelz, E., Huffaker, A., Holton, N., Zipfel, C., & Doehlemann, G. (2018). An apoplastic peptide activates salicylic acid signalling in maize. *Nature Plants*, *4*(3), Article 3. https://doi.org/10.1038/s41477-018-0116-y